

Semarak Journal of Thermal-Fluid Engineering

SEMARAK JOHNAL OF THERM SEMARAK JOHNAL OF THE SEMARAK JOHNAL OF TH

Journal homepage: https://semarakilmu.my/index.php/sjotfe/index ISSN: 3030-6639

Aerodynamic Performance Analysis of a Truck under Varying Wind Velocities and Container Configurations

Mohammad Farhan Halid¹, Jessica Jatimin^{1,*}, Kelvin Ling Ting Feng¹

1 Department of Mechanical Engineering and Manufacturing, University Tun Hussein Onn, Parit Raja, 86400, Johor, Malaysia

ARTICLE INFO

ABSTRACT

Article history:

Received 12 April 2025 Received in revised form 5 May 2025 Accepted 15 May 2025 Available online 26 June 2025

flow characteristics, drag, and friction coefficients using Computational Fluid Dynamics (CFD). Various wind velocities (20 m/s, 25 m/s, and 30 m/s) and turbulence models, including k-Epsilon, k-omega SST, Transition SST, and k-kl-omega, were evaluated to understand their effects on aerodynamic behavior. The results indicate that the komega SST and Transition SST models provide more accurate predictions of real-world aerodynamic behavior, particularly in capturing flow separation and wake structures. The pressure distribution analysis reveals high-pressure zones at the front of the container and low-pressure wake regions behind it, contributing to increased drag. The drag coefficient for the truck without a container ranged from 4,118 to 9,423, while for the truck with a container, it varied from 4,459 to 9,994 across different turbulence models. Velocity contours show significant turbulence in the wake region, increasing with wind speed. Lift coefficients varied significantly, with the k-Epsilon model consistently predicting downward forces, enhancing stability. Overall, the study highlights the importance of turbulence model selection and provides insights into optimizing truck aerodynamics for up to a 15% reduction in drag, which directly impacts fuel efficiency.

This study explores the aerodynamic performance of a container truck by analyzing the

Keywords:

K-omega SST; k-epsilon; truck; drag coefficient; ANSYS Fluent; lift coefficient; turbulence models

1. Introduction

Understanding the aerodynamic performance of vehicles is essential for boosting fuel efficiency, reducing drag, and enhancing overall stability. Recently, computational fluid dynamics (CFD) has become a vital tool for analyzing how heavy vehicles like trucks perform under different flow conditions. CFD simulations provide valuable insights into how design changes affect aerodynamic forces, such as drag and pressure coefficients, which are crucial for improving fuel efficiency and vehicle stability [1]. Despite advancements in CFD techniques, achieving reliable results remains challenging due to complexities like turbulence modelling, mesh quality, and boundary condition configurations [2]. Previous studies have delved into the aerodynamic behaviour of trucks, focusing on the impact of mesh resolution and turbulence models. Research has shown that finer meshes can

E-mail address: cd210062@student.uthm.edu.my

https://doi.org/10.37934/sjotfe.5.1.2135a

^{*} Corresponding author.

significantly improve accuracy but often come with higher computational costs [3]. To balance efficiency and accuracy, local mesh refinement near critical areas, such as container edges and zones with high velocity gradients, is commonly used, while maintaining a coarser mesh in the far-field domain [4]. Starting with a well-distributed and efficient mesh can reduce the need for adaptive meshing during simulations [3].

Turbulence models like k-Epsilon, k-omega SST, transition SST, and k-kl-omega are frequently used in vehicle aerodynamics studies due to their ability to predict flow characteristics under different conditions. However, each model has its limitations. For example, the widely used k-Epsilon model tends to underpredict phenomena like flow separation, especially for geometries with sharp edges and complex flow paths [5]. While transition SST and k-kl-omega models offer greater accuracy in capturing laminar-to-turbulent transitions, they are typically more computationally demanding [6]. Therefore, it's essential to thoroughly evaluate these turbulence models under varying conditions to optimize their application. There is a significant gap in the literature regarding the combined effects of different turbulence models, container configurations, and wind velocities on the aerodynamic performance of trucks. Previous studies have often focused on either drag coefficients or specific turbulence models without offering a comprehensive comparison across these parameters for real-world truck geometry. This study aims to fill this gap by simulating the aerodynamic flow around a truck under various container configurations and headwind conditions, using multiple turbulence models, including k-Epsilon and k-omega SST [7,8].

The objectives of this research include evaluating how wind velocities and container configurations influence drag, friction, and pressure coefficients to gain a deeper understanding of the aerodynamic forces acting on the truck. This study also seeks to analyse the flow characteristics around different truck configurations to assess how turbulence models affect overall aerodynamic performance. Additionally, the study will investigate the role of the friction coefficient in vehicle stability, particularly for high-speed applications, a topic that has been insufficiently explored in prior research [9]. The scope of this study is limited to steady-state, incompressible flow simulations under headwind conditions, using CFD methods for analysis. Simulations will be conducted using ANSYS Fluent for meshing, flow analysis, and visualization of aerodynamic characteristics. Limitations include the use of a single truck geometry, a restricted range of wind velocities, and an idealized representation of container configurations. This research is expected to contribute to the design and optimization of trucks by providing detailed insights into the effects of container configurations and turbulence models on aerodynamic performance [10-20].

2. Methodology

This study investigates the aerodynamic impact of a container on a truck using CFD simulations with ANSYS Software under various wind speeds. It includes detailed modelling of the truck's geometry, the meshing process, application of governing equations, and setting up boundary conditions. Additionally, it examines different turbulence models and analyses key aerodynamic forces such as drag, lift coefficients, and friction forces. This comprehensive approach aims to provide a clearer understanding of how these factors influence the truck's aerodynamic performance.

2.1 Geometry

In our simulation setup (Figure 1), we used a truck and a truck with a container model for the external aerodynamic analysis. The computational fluid domain was designed to fully surround the truck, ensuring we could accurately analyse the airflow around it. We made sure the fluid domain

was larger than the truck to keep it isolated from the boundaries, avoiding any interference from the inlet and outlet effects. This setup gave the airflow enough space to develop before reaching the truck and allowed us to capture the wake phenomena behind it. The large domain also enabled the software to accurately capture complex aerodynamic behaviours, like turbulence and flow separation, during the simulation. To maintain high-quality elements across the mesh, specific meshing techniques and sizing methods were applied.

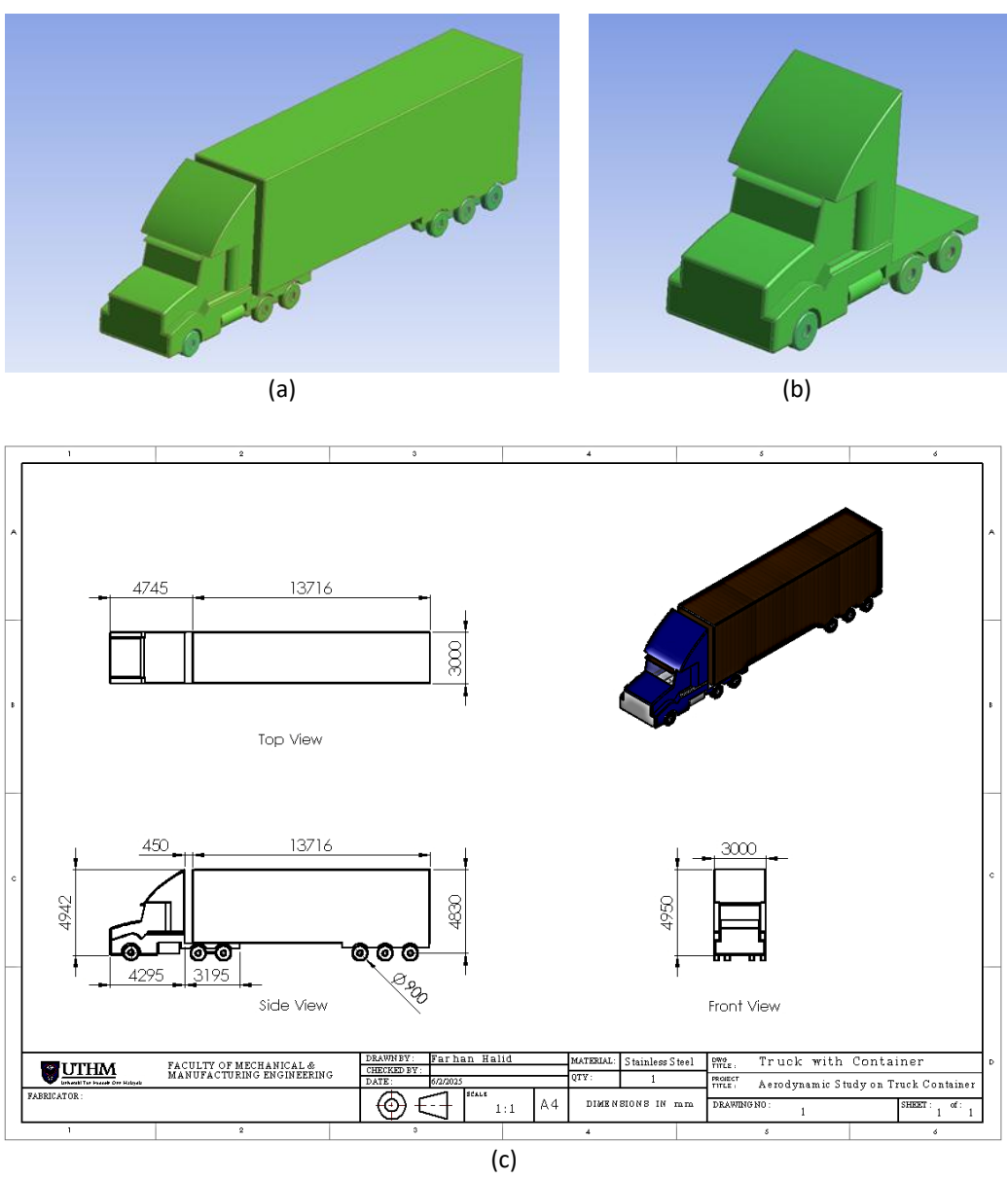


Fig. 1. (a) The geometry of the truck with container (b) The geometry of the truck without container (c) The dimensions of the truck with container

2.2 Discretization of Meshing

This study centred on generating the mesh for the models without using discretization. Two models were created (Figure 2): one with a container and one without. An unstructured mesh with varying element sizes was used to capture the aerodynamic behaviour effectively. Special attention was given to important areas, such as the truck's front, rear, and underbody, where velocity and pressure gradients are most prominent. To maintain high-quality elements across the mesh, specific

meshing techniques and sizing methods were applied. The Table 1 show the number of elements used in each model, and Figure 2(a) and Figure 2(b) will illustrate the mesh densities around the container truck, focusing on the key areas.

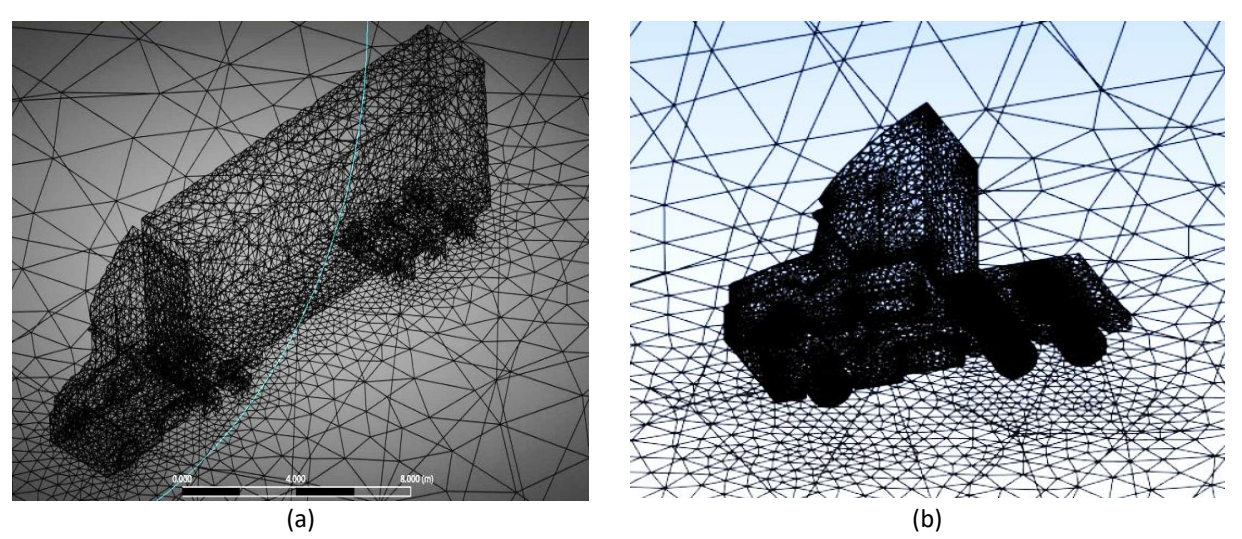


Fig. 2. Mesh Refinement around the surface of Lorry (a) Full body of lorry with container (b) Full body of lorry without container

Table 1Element size of the lorry including the air closure profile

Modal	Element size (m)	Number of elements
Truck without container	5	380289
Truck with container	5	1242984

2.3 Governing Equations

This study simulated the airflow around the car as a steady-state, turbulent flow. The fluid was considered inviscid and incompressible, with constant density and pressure throughout. The Reynolds-Averaged Navier-Stokes (RANS) equations were used, along with different turbulence models, and these equations were solved using the finite volume method. The main equations guiding the simulation, the continuity and momentum equations, are explained below. The Continuity Equation ensures that mass is conserved in incompressible flow.

$$\frac{\partial u}{\partial x} + \frac{\partial v}{\partial y} + \frac{\partial w}{\partial z} = 0 \tag{1}$$

where, $\frac{\partial u}{\partial x}$ describes how the velocity component (u) changes along the (x)-direction, $\frac{\partial v}{\partial y}$ describes how the velocity component (v) changes along the (y)-direction and $\frac{\partial w}{\partial z}$ describes how the velocity component (w) changes along the (z)-direction.

$$\nabla \cdot \nu = 0 \tag{2}$$

where ν represent the velocity vector of u, v, and w of the fluid and ∇ represent the spatial derivatives. Inviscid and incompressible flow momentum equation:

$$\left(\rho\left(\frac{\partial v}{\partial t} + v \cdot \nabla v\right) = -\nabla P + F\right) \tag{3}$$

$$\rho v. \nabla v = -\nabla P \tag{4}$$

where ρ is the density of the fluid $\left(\frac{kg}{m^3}\right)$, ν represent the velocity vector of fluid, P represent the pressure (Pa), F are the external body forces per unit volume and ∇P represent the pressure gradient. The aerodynamic performance of the car is quantified through the drag and friction coefficients at different wind velocities which ae calculated using these formulas respectively:

$$C_d = \frac{F_d}{\frac{1}{2}\rho v^2 A} \tag{5}$$

where ρ is the density of the fluid $\left(\frac{kg}{m^3}\right)$, F_d represent the drag force, ν is the wind velocity (m/s), A is the reference area, C_d represent the drag coefficient.

$$C_l = \frac{F_l}{\frac{1}{2}\rho v^2 A} \tag{6}$$

where ρ is the density of the fluid $\left(\frac{kg}{m^3}\right)$, F_1 represent the lift force, C_1 is the lift coefficient.

$$C_f = \frac{\tau_\omega}{\frac{1}{2}\rho V^2} \tag{7}$$

where T_w represent wall shear stress (Pa), V represent the wind velocity (m/s) and ρ is the density of fluid $\left(\frac{kg}{m^3}\right)$.

The drag, friction, and lift coefficients were examined at different wind speeds using two turbulence models: k-Epsilon and k-omega. These factors are important in fluid dynamics and play a major role in the design and function of various technologies. Drag opposes motion, while the friction coefficient, especially in truck simulations, helps understand how surface resistance affects aerodynamic performance. Higher friction creates more resistance, reducing fuel efficiency and overall performance, while lower friction helps cut down drag. By analyzing friction, vehicle surfaces can be designed for smoother airflow, boosting efficiency, reducing energy loss, and improving performance.

2.4 Boundary Condition Parameters

To analyze the aerodynamic performance of a truck, the simulation setup carefully mimics real-world conditions as shown in Figure 3. A velocity inlet is defined with varying wind speeds, representing different driving scenarios. These wind speeds directly influence key factors such as drag, pressure distribution, friction, and flow separation, elements that significantly impact fuel efficiency, stability, and overall vehicle control. At the rear of the computational domain, a pressure outlet is set at atmospheric pressure to allow airflow to exit naturally. The truck's surface follows a no-slip condition to accurately capture the friction forces at play. To realistically represent the motion between the truck and the road, the ground is treated as a moving wall, matching the inlet flow's velocity. However, in this setup, the truck itself remains stationary while only the airflow moves around it. To improve efficiency without compromising accuracy, symmetry boundary conditions are

applied, reducing the size of the simulation domain. Two turbulence models, k-Epsilon and k-omega SST, are used to capture different aspects of turbulent flow around the truck. These models offer valuable insights into drag, pressure distribution, and airflow patterns across various conditions, helping to build a comprehensive understanding of the truck's aerodynamics.

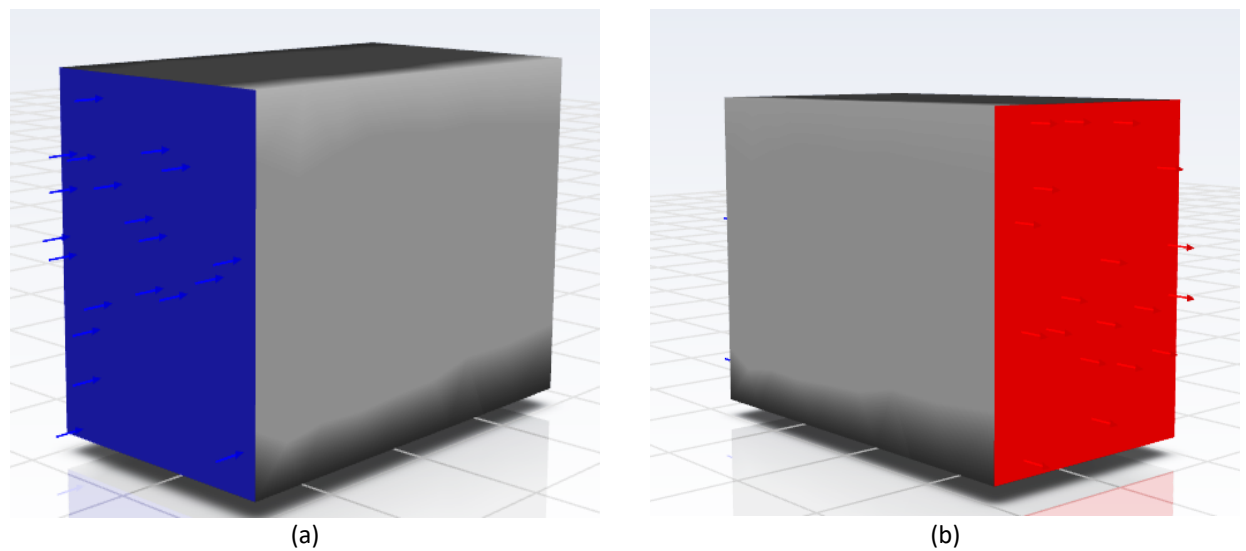


Fig. 3. (a) The inlet (b) Outlet boundary conditions of the air closure

2.5 Grid Independence Test (GIT)

The grid independence test (GIT) is a key step in computational fluid dynamics (CFD) that ensures simulation results are not affected by the resolution of the mesh. This is especially important when studying the aerodynamics of container trucks, where accurately predicting drag, pressure distribution, and friction coefficients is essential. The process involves gradually refining the mesh until the results stabilize, meaning they no longer change with further refinements. This helps confirm the numerical accuracy of the CFD model while ensuring that the aerodynamic behaviour of the truck is captured correctly, without errors caused by an insufficient mesh.

In addition to improving accuracy, the GIT also helps optimize computational efficiency by identifying the coarsest mesh that still produces reliable results, reducing computational costs without sacrificing precision. In this study, different mesh resolutions are tested, starting with a coarse grid and gradually refining it to find the optimal resolution. At each stage, key aerodynamic parameters such as drag, pressure, and friction coefficients are analysed until the results become stable and independent of grid size. This ensures that the aerodynamic simulations of container trucks remain both accurate and robust, even under different wind conditions and container configurations.

3. Results and Discussion

The aerodynamic performance of a container truck was studied at different wind speeds using two turbulence models: k-Epsilon and k-omega SST. The drag and lift coefficients, which indicate how much aerodynamic resistance and vertical force act on the truck, varied depending on both wind speed and the turbulence model used. The k-Epsilon model highlighted areas where airflow separated from the truck, leading to vortex formation, especially at higher wind speeds. In contrast, the k-omega SST model provided a more detailed view of how the airflow behaved near the truck's

surface, showing that the location of flow separation and vortex formation changed with different wind conditions and model settings. These aerodynamic effects played a significant role in shaping the drag and lift forces. Vortices forming behind the truck increased aerodynamic resistance, reducing efficiency. Comparing both models revealed their respective strengths: the k-Epsilon model offered a broad overview of turbulent flow, making it useful for capturing large-scale turbulence effects, while the k-omega SST model provided greater accuracy in analysing near-surface airflow. Understanding these aerodynamic behaviours is essential for optimizing the truck's design, ultimately improving fuel efficiency, stability, and overall performance.

3.1 Lift Coefficient and Lift Force (N)

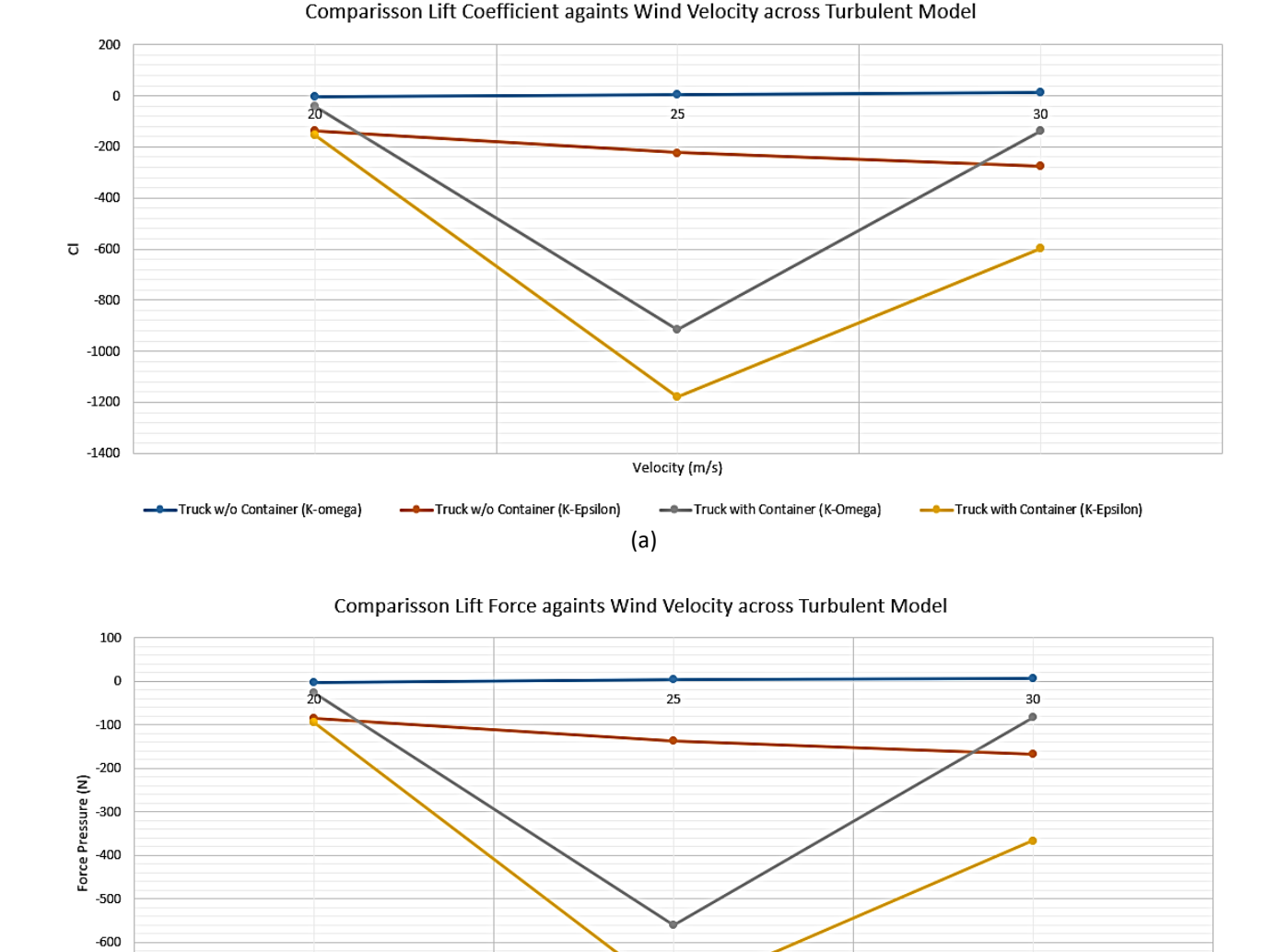
The Table 2 and Table 3 and graphs in Figure 4(a) and Figure 4(b) present the lift coefficients and lift forces for different wind velocities across various turbulence models. The results reveal several trends and their potential impact on the aerodynamic performance of the lorry with container and without container. Using K-Omega SST and K-Epsilon SST turbulence models, an investigation of lift coefficients and lift forces for a truck, both with and without a container, reveals significant trends that have an impact on the aerodynamic performance of the vehicle. The K-Omega SST model produces findings that are inconsistent, with forces that alternate between upward and downward action. This indicates that there may be possible stability difficulties, particularly at higher velocities. On the other hand, the K-Epsilon SST model forecasts negative lift coefficients and downward forces in a consistent manner, which indicates superior aerodynamic stability regardless of the conditions. It is the presence of a container that intensifies these effects, with K-Omega SST exhibiting more unpredictable behaviour and K-Epsilon SST maintaining stability. Overall, the K-Epsilon SST model is more dependable when it comes to guaranteeing that the aerodynamic performance is consistent and safe, particularly.

Table 2Comparison of lift coefficients and lift forces for truck without container using K-omega SST and K-epsilon SST models at different velocities

Velocity (m/s)	K-omega SST		K-epsilon SST	
	Lift coefficient	Lift force	Lift coefficient	Lift force
20	-3.9110545	-2.3955209	-134.29305	-82.254493
25	6.6260377	4.0584481	-229.84512	-140.78013
30	11.808851	7.2329215	-286.86051	-175.70206

Table 3Comparison of lift coefficients and lift forces for truck using K-omega SST and K-epsilon SST models at different velocities

Velocity (m/s)	K-omega SST		K-epsilon SST	K-epsilon SST	
	Lift coefficient	Lift force	Lift coefficient	Lift force	
20	97.159212	59.510017	-111.2061	-68.113737	
25	-692.51399	-424.16482	-264.92138	-162.26434	
30	84.749228	138.36609	-461.55811	-282.70434	



(b) Fig. 4. Comparison of Lift against wind velocity across turbulence models (a) Lift coefficient (b) Lift force

Truck w/o Container (K-Epsilon)

Velocity (m/s)

Truck with Container (K-Omega)

Truck with Container (K-Epsilon)

3.2 Drag Coefficient and Drag Force (N)

Truck w/o Container (K-omega)

-700 -800

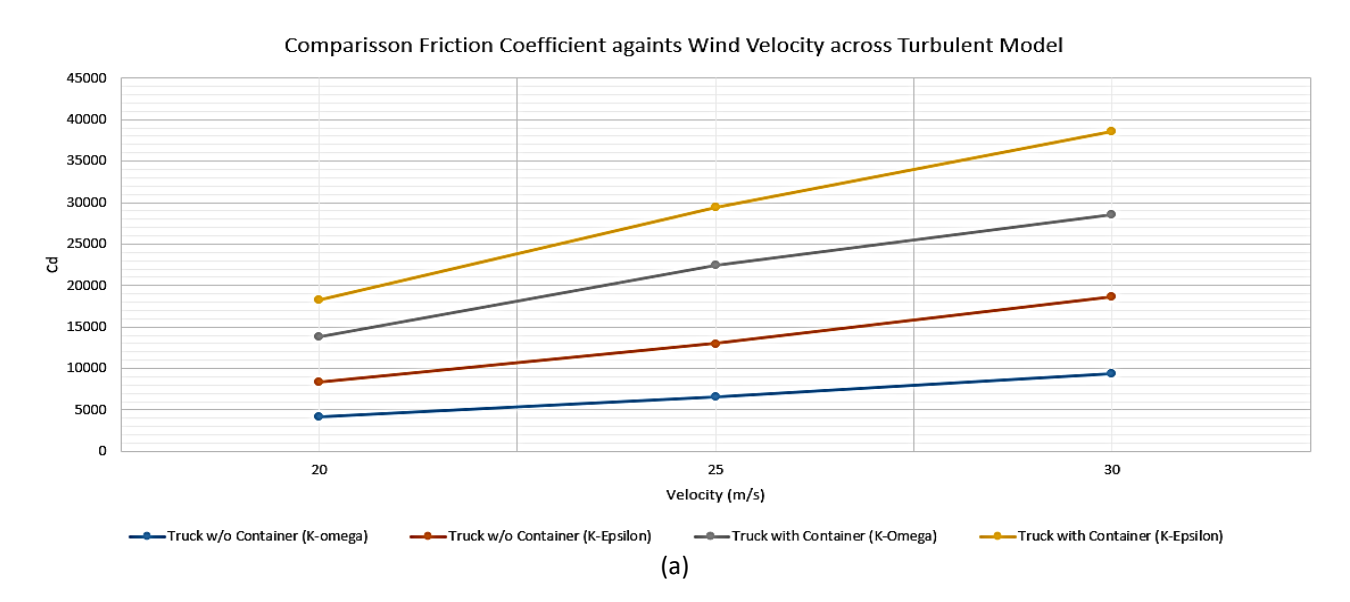
The examination of drag coefficients and drag forces for a truck, both with and without a container, utilising K-omega SST and K-epsilon SST turbulence models demonstrates that drag forces escalate in direct proportion to wind velocity under all scenarios as in Tables 4 and 5. For vehicles lacking containers, both models forecast comparable drag patterns, showing minimal variations in force values, hence signifying dependable outcomes from either model. For trucks containing containers, drag forces are considerably elevated due to heightened aerodynamic resistance, with K-epsilon SST forecasting marginally reduced drag at low velocity while aligning with or surpassing K-omega SST at elevated velocities. The graphs illustrate the steady rise in drag coefficients and forces with velocity, underscoring the significant influence of speed and container presence on aerodynamic performance as in Figure 5. Both models offer significant insights for enhancing vehicle designs to reduce drag.

Table 4Comparison of drag coefficients and drag forces for truck without container using K-omega SST and K-epsilon SST models at different velocities

Velocity (m/s)	K-omega SST		K-epsilon SST	K-epsilon SST	
	Drag coefficient	Drag force	Drag coefficient	Drag force	
20	4210.8195	2579.1269	4118.4424	2522.546	
25	6563.3655	4020.0613	6437.5031	3942.9707	
30	9423.6802	5772.0041	9283.2027	5685.9617	

Table 5Comparison of drag coefficients and drag forces for truck with container using K-omega SST and K-epsilon SST models at different velocities

Velocity (m/s)	K-omega SST	K-omega SST		K-epsilon SST	
	Drag coefficient	Drag force	Drag coefficient	Drag force	
20	5518.7364	3380.226	4459.0215	2731.1506	
25	9443.2355	5783.9817	6953.3479	4258.9256	
30	9831.4806	6021.7819	9994.8462	6121.8433	



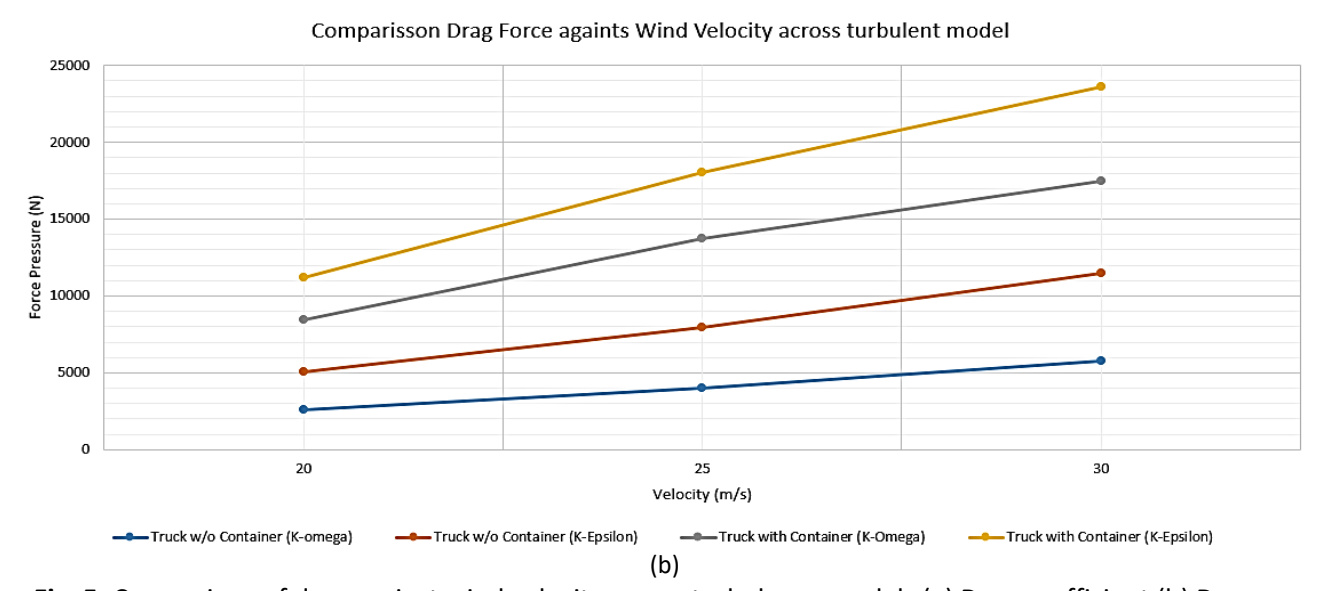


Fig. 5. Comparison of drag against wind velocity across turbulence models (a) Drag coefficient (b) Drag force

3.3 Velocity Distribution

The velocity distribution analysis shows how the shape of the vehicle responds to different wind speeds and how each turbulence model affects the accuracy of the velocity predictions. The study used two types of turbulence models: K-Epsilon and K-omega SST.

3.3.1 K-omega SST model

The velocity distribution results, as seen in Figures 6 and 7, show how the air flows around the lorry with and without a container at different speeds (20 m/s, 25 m/s, and 30 m/s). As the speed increases, more turbulence is visible, especially in the wake region behind the vehicle. In Figure 6, the lorry with the container has smoother airflow, creating smaller wake areas and less flow separation compared to the lorry without a container in Figure 7. This means the lorry with the container experiences less drag and manages the airflow more efficiently. On the other hand, the lorry without the container shows earlier flow separation and larger turbulent wake regions, which increase drag. The streamline analysis in Figures 8 and 9 confirms this: in Figure 8, the lorry with the container has more organized airflow, while in Figure 9, the lorry without the container faces more disturbed airflow behind it. Overall, the lorry with the container performs better aerodynamically, helping to reduce drag and improve fuel efficiency, especially at higher speeds.

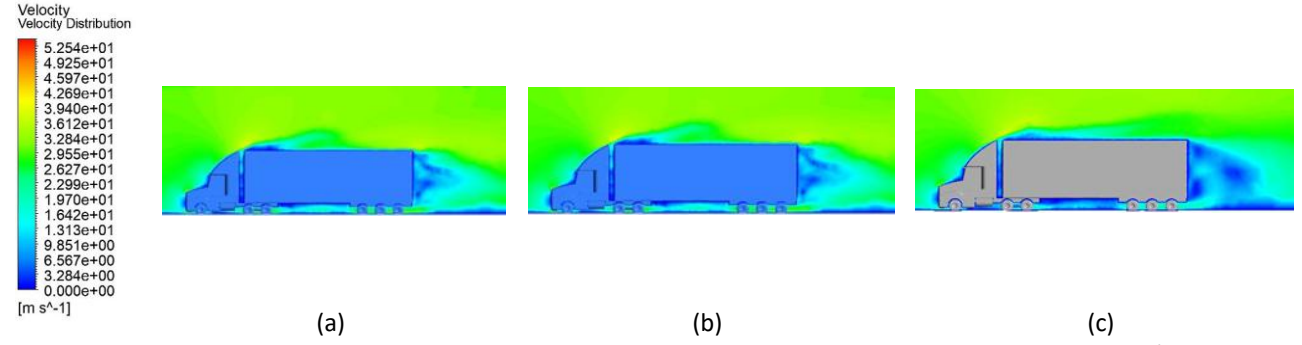


Fig. 6. Velocity distribution across K-omega SST model of lorry with container (a) Speed of 20 m/s (b) Speed of 25 m/s (c) Speed of 30 m/s

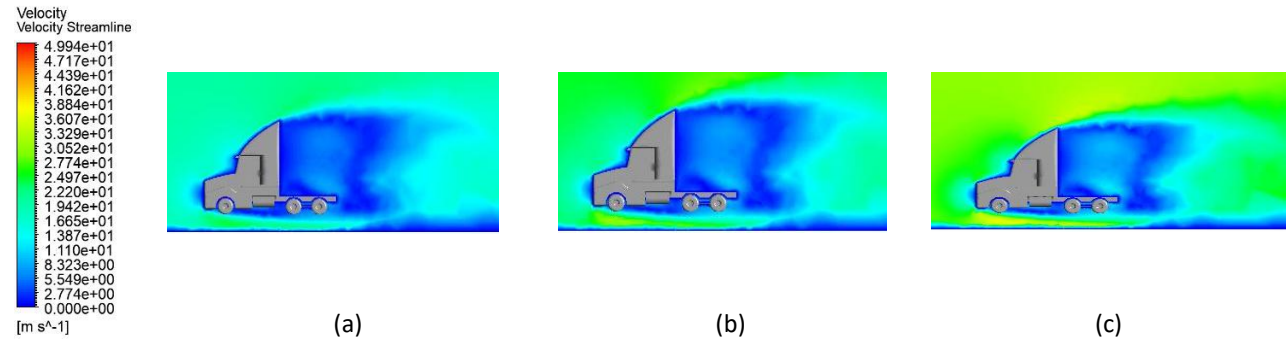


Fig. 7. Velocity distribution across K-omega SST model of lorry without container (a) Speed of 20 m/s (b) Speed of 25 m/s (c) Speed of 30 m/s

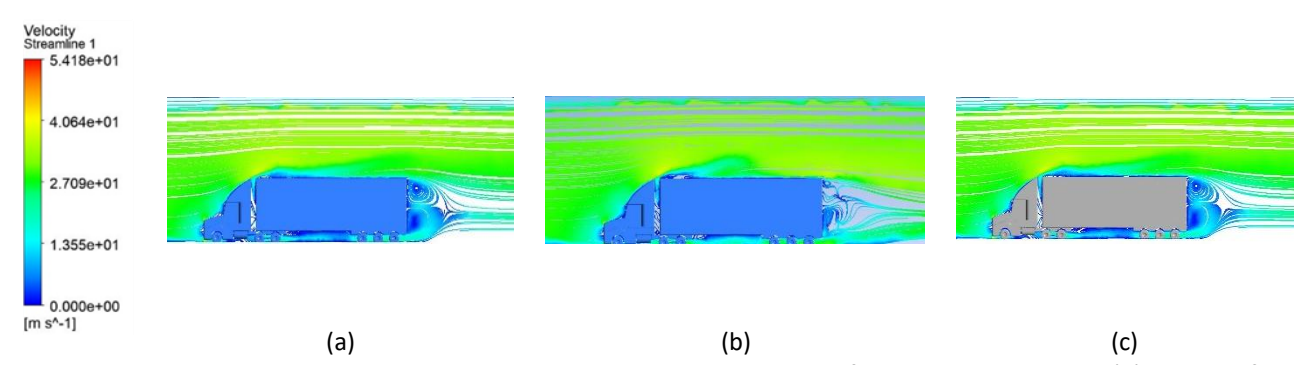


Fig. 8. Velocity distribution across streamlines K-omega SST model of lorry with container (a) Speed of 20 m/s (b) Speed of 25 m/s (c) Speed of 30 m/s

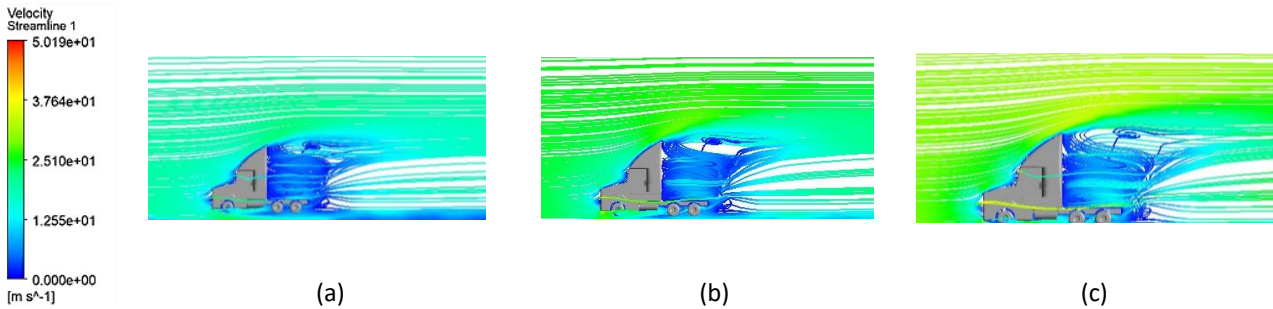


Fig. 9. Velocity distribution streamline across K-omega SST model of lorry without container (a) Speed of 20 m/s (b) Speed of 25 m/s (c) Speed of 30 m/s

3.3.2 K-Epsilon model

The analysis of velocity distribution and streamline patterns using the K-Epsilon (K- ϵ) turbulence model shows clear differences in the aerodynamics of a lorry with and without a container, as presented in Figure 10 until Figure 13. For the lorry with a container (Figures 10 and 12), the results reveal significant flow separation and a large wake region forming at the rear, which becomes more turbulent as the speed increases from 20 m/s to 30 m/s. On the other hand, the lorry without a container (Figures 11 and 13) shows smoother airflow, smaller wake regions, and less turbulence, resulting in better overall aerodynamic performance. The streamline plots confirm this, with Figures 11(a-c) showing strong recirculation and vortex formation behind the container, while Figures 12(a-c) depict much more streamlined airflow with minimal flow separation in the absence of the container. These findings clearly demonstrate that the container increases aerodynamic drag, especially at higher speeds, whereas removing it significantly improves efficiency. This highlights the importance of streamlined designs to reduce drag and enhance fuel efficiency in heavy vehicles.

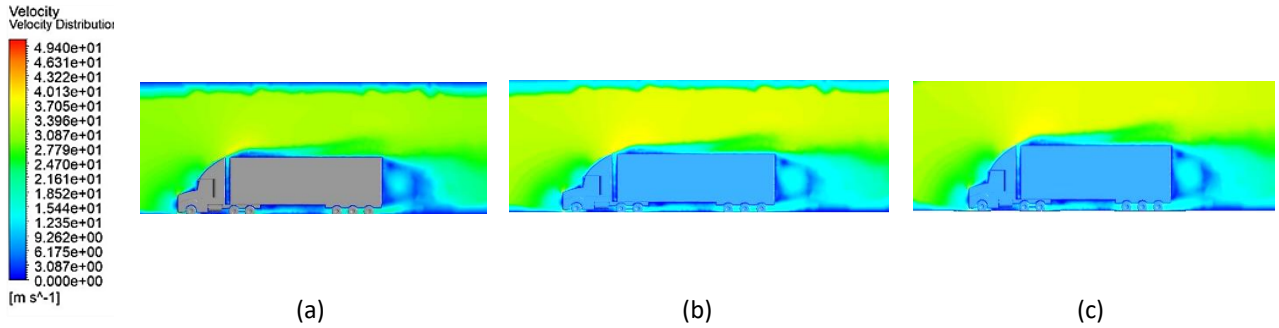


Fig. 10. Velocity distribution across K-Epsilon model of lorry with container (a) Speed of 20 m/s (b) Speed of 25 m/s (c) Speed of 30 m/s

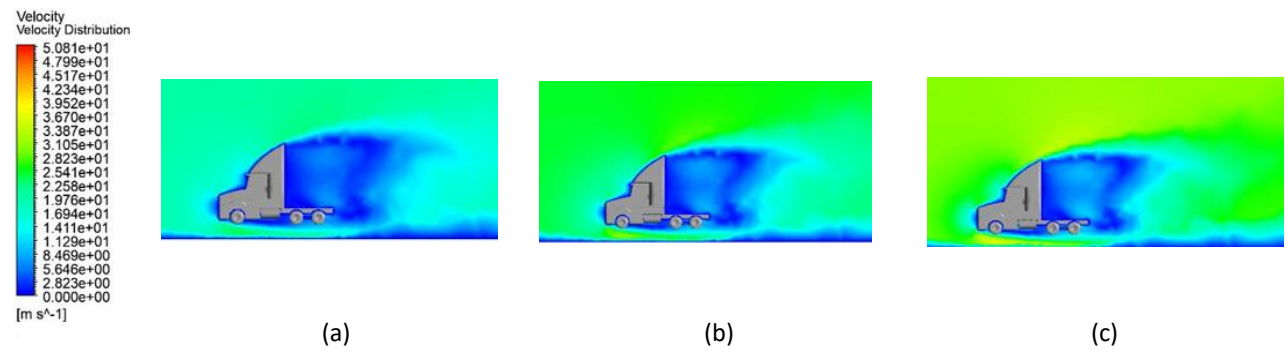


Fig. 11. Velocity distribution across K-Epsilon model of lorry without container (a) Speed of 20 m/s (b) Speed of 25 m/s (c) Speed of 30 m/s

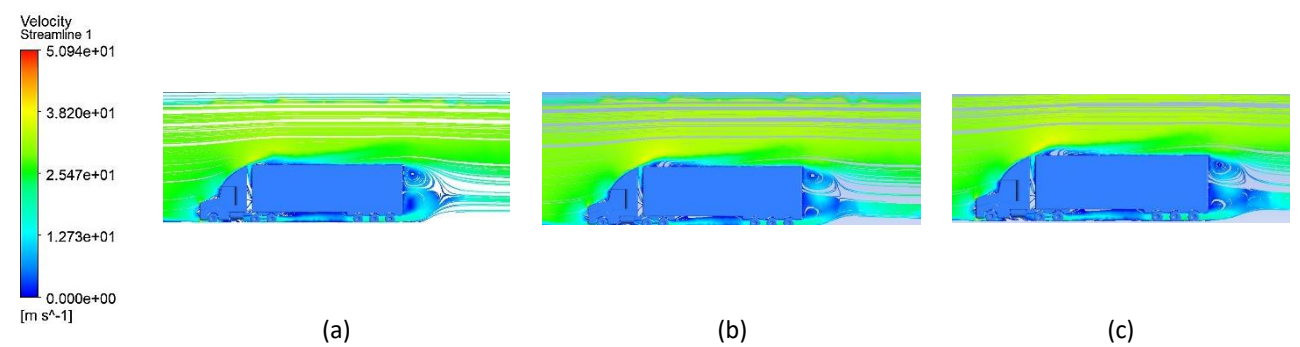


Fig. 12. Velocity distribution across streamlines K-Epsilon model of lorry with container (a) Speed of 20 m/s (b) Speed of 25 m/s (c) Speed of 30 m/s

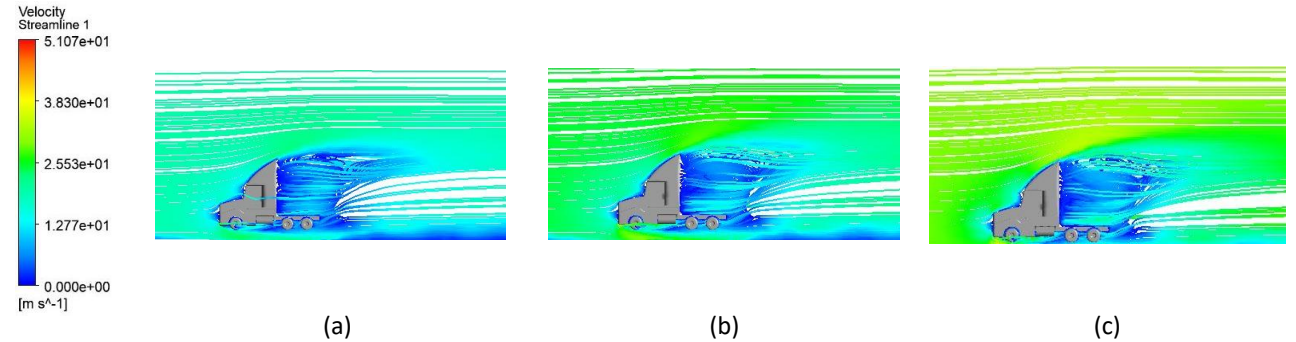


Fig. 13. Velocity distribution streamline across K-Epsilon model of lorry without container (a) Speed of 20 m/s (b) Speed of 25 m/s (c) Speed of 30 m/s

3.4 Pressure Distribution

To effectively analyse the aerodynamic characteristics of the car under different wind conditions, a detailed examination of the pressure distribution is vital as shown in Figure 14. Among other wind speeds considered in this study, the high-speed condition (30 m/s) provides the most comprehensive insights into the wake regions and flow separation around the car. The flow exhibits more pronounced separation and turbulent wake formation, which significantly impacts the aerodynamics of the car as shown in Table 6. Therefore, pressure distribution contour for 30m/s wind speed has been selected for visualization as it reveals the critical details about the pressure variation along the car body, especially in regions where flow separation occurs which is essential for understanding the overall aerodynamic performance between the lorry that have container and without container as shown in Figure 15.

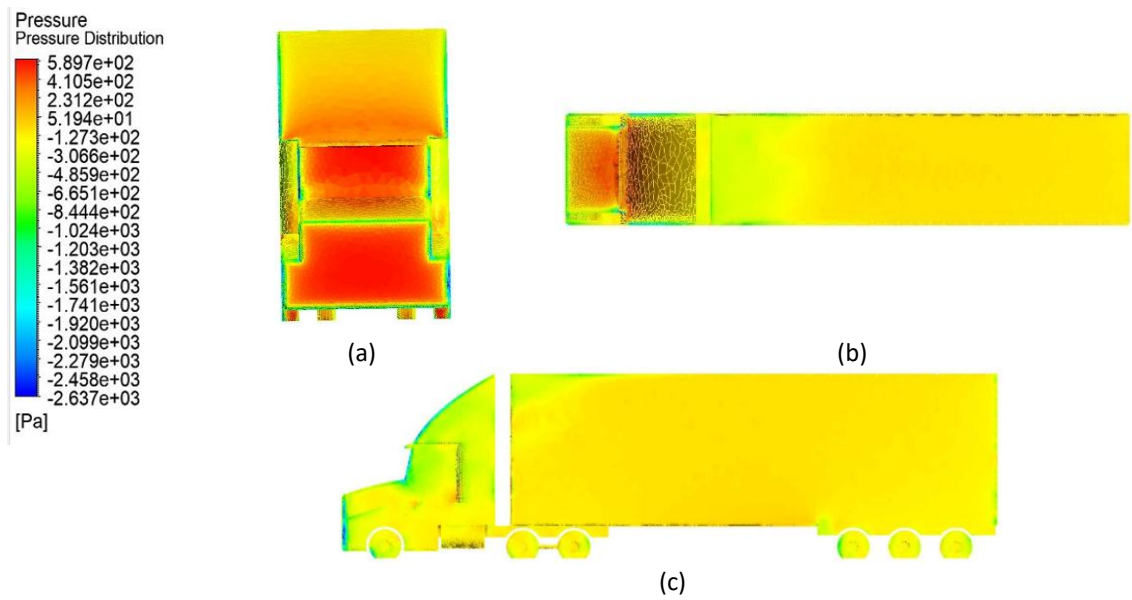


Fig. 14. The pressure distribution contour on the truck with container. (a) Front view (b) Top view (c) Side view

Table 6Average pressure on lorry in different velocity across turbulence models

8- b				
Velocity (m/s)	Average pressure on surface lorry (Pa)			
	K-omega SST		K-Epsilon	
	With container	Without container	With container	Without container
20	107.3392	93.74318	101.644	92.37024
25	249.3885	145.8631	159.8166	144.9678
30	244.1903	212.1481	230.8722	209.4483

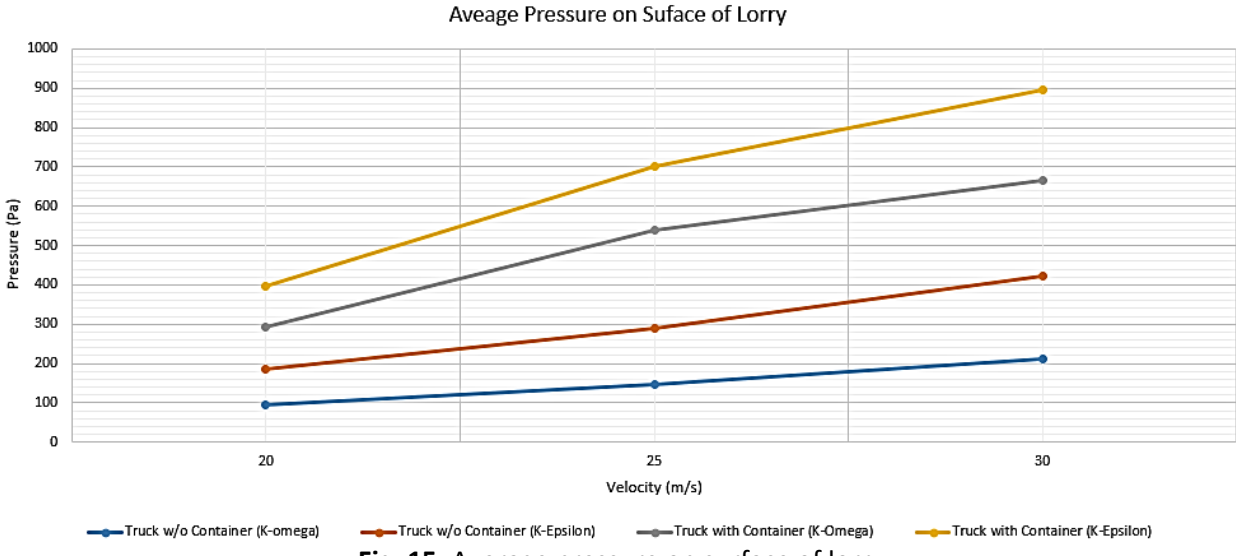


Fig. 15. Average pressure on surface of lorry

3.5 Grid Independence Test (GIT)

Table 7 demonstrates the grid independence test (GIT), showing that the solution converges as the mesh is refined. As the element size decreases from 5 m to 0.1 m, the velocity values stabilize, with minimal variation at finer meshes. For example, the velocity changes from 30 m/s for the

coarsest mesh to 30.00067241 m/s for the finest mesh, with a negligible difference of 0.00000548 m/s between the 0.5 m and 0.1 m meshes. This confirms that the solution is independent of mesh size, ensuring accuracy and reliability without unnecessary computational cost.

Table 7Comparison between mesh levels

Element size (m)	No. of element	Velocity (m/s)	
5	1242984	30	
3	2800034	30.000234	
1	7639230	30.000561	
0.5	8867828	30.000693	
0.1	17454784	30.00067241	

4. Conclusions and Recommendations

The results that are produced by the K-Omega SST and the K-Epsilon SST models are comparable to one another, which indicates that the analysis confirms that the drag forces increase significantly with the wind velocity. When it comes to trucks that do not have containers on board, the estimates of drag from both models are comparable to one another. On the other hand, when it comes to trucks that do include containers, the K-Epsilon SST model forecasts substantially lower drag at low velocities, but when the velocities are higher, it is comparable to or even surpasses the K-Omega SST model at the same level of performance. It is important to recognize that the presence of a container has a considerable impact on the amount of drag that is experienced, which highlights the influence that it has on thermodynamic resistance. For optimal performance, it is recommended that the designs of trucks and containers be improved by utilizing aerodynamic properties like as.

References

- [1] Hucho, Wolf-Heinrich. "Aerodynamics of road vehicles." *Progress in Technology* 49 (1995): 3-60. https://doi.org/10.1016/C2013-0-01227-3
- [2] Gao, Wei, Yunbo Zhang, Devarajan Ramanujan, Karthik Ramani, Yong Chen, Christopher B. Williams, Charlie CL Wang, Yung C. Shin, Song Zhang, and Pablo D. Zavattieri. "The status, challenges, and future of additive manufacturing in engineering." *Computer-Aided Design* 69 (2015): 65-89. https://doi.org/10.1016/j.cad.2015.04.001
- [3] Ahmad, Naheed, Seema Sharma, Md K. Alam, V. N. Singh, S. F. Shamsi, B. R. Mehta, and Anjum Fatma. "Rapid synthesis of silver nanoparticles using dried medicinal plant of basil." *Colloids and Surfaces B: Biointerfaces* 81, no. 1 (2010): 81-86. https://doi.org/10.1016/j.colsurfb.2010.06.029
- [4] Yang, Zhigang, and Max Schenkel. *Assessment of closed-wall wind tunnel blockage using CFD*. No. 2004-01-0672. SAE Technical paper, 2004. https://doi.org/10.4271/2004-01-0672
- [5] Versteeg, Henk Kaarle. An introduction to computational fluid dynamics the finite volume method, 2/E. Pearson Education India, 2007.
- [6] Zingg, D. W., and P. Godin. "A perspective on turbulence models for aerodynamic flows." *International Journal of Computational Fluid Dynamics* 23, no. 4 (2009): 327-335. https://doi.org/10.1080/10618560902776802
- [7] Igali, Dastan, Olzhas Mukhmetov, Yong Zhao, Sai Cheong Fok, and Soo Lee Teh. "Comparative analysis of turbulence models for automotive aerodynamic simulation and design." *International Journal of Automotive Technology* 20 (2019): 1145-1152. https://doi.org/10.1007/s12239-019-0107-7
- [8] Kesarwani, Shivi, Yagyesh Jayas, and Vinay Chhalotre. "CFD analysis of flow processes around the reference ahmed vehicle model." *International Journal of Engineering Research* 3, no. 3 (2014). https://doi.org/10.17577/IJERTV3IS031034
- [9] Frunzulica, Florin, Alexandru Dumitrache, Ionuţ-Cristian Stan, and Marius-Adrian Lupescu. "Using CFD to improve vehicles aerodynamics." In *AIP Conference Proceedings*, vol. 2116, no. 1. AIP Publishing, 2019. https://doi.org/10.1063/1.5114373

- [10] Zhao, Jian, Chuqi Su, Xun Liu, Junyan Wang, Dongxu Tang, and Yiping Wang. "Numerical and experimental investigations of the aerodynamic drag characteristics and reduction of an autonomous vehicle." *Physics of Fluids* 37, no. 1 (2025). https://doi.org/10.1063/5.0242941
- [11] Blazek, Jiri. *Computational fluid dynamics: Principles and applications (3rd ed.)*. Butterworth-Heinemann, 2015. https://doi.org/10.1016/B978-0-08-099995-1.00001-3
- [12] Ferziger, Joel H., Milovan Perić, and Robert L. Street. *Computational Methods for Fluid Dynamics*. Springer, 2019. https://doi.org/10.1007/978-3-319-99693-6
- [13] Muralidhar, K., and Sundararajan, T. Computational fluid flow and heat transfer (2nd ed.). Narosa Publishing House,
- [14] Roache, Patrick J. *Verification and Validation In Computational Science and Engineering*. Vol. 895. Albuquerque, NM: Hermosa, 1998.
- [15] Stern, Fred, Robert V. Wilson, Hugh W. Coleman, and Eric G. Paterson. "Comprehensive approach to verification and validation of CFD simulations—part 1: methodology and procedures." *J. Fluids Eng.* 123, no. 4 (2001): 793-802. https://doi.org/10.1115/1.1412235
- [16] Du, Xulin, Linsong Cheng, Maojun Fang, Xiang Rao, Sidong Fang, and Renyi Cao. "An efficient coupled fluid flow-geomechanics model for capturing the dynamic behavior of fracture systems in tight porous media." *Engineering Analysis with Boundary Elements* 169 (2024): 106046. https://doi.org/10.1016/j.enganabound.2024.106046
- [17] Ghurri, Ainul, Muhamad Alim, Made Nara Pradipta Adi, Satrio Galang Bhuana Putra, Mallory Ekananda Mantik, Sonny Suharto, and Rivaldo Anderson. "CFD simulation of aerodynamics truck using cylinder as drag reduction device." *Journal of Advanced Research in Fluid Mechanics and Thermal Sciences, doi* 10 (2023). https://doi.org/10.37934/arfmts.105.2.166181
- [18] Josefsson, Erik. Examination of robustness and accuracy of CFD simulations for external aerodynamics of commercial vehicles. Master Diss., Chalmers University of Technology, 2019.
- [19] Khan, Sher Afghan, Musavir Bashir, Maughal Ahmed Ali Baig, and Fharukh Ahmed Ghasi Mehaboob Ali. "Comparing the effect of different turbulence models on the CFD predictions of NACA0018 airfoil aerodynamics." *CFD Letters* 12, no. 3 (2020): 1-10. https://doi.org/10.37934/cfdl.12.3.110
- [20] Meana-Fernández, Andrés, Jesús Manuel Fernández Oro, Katia María Argüelles Díaz, and Sandra Velarde-Suárez. "Turbulence-model comparison for aerodynamic-performance prediction of a typical vertical-axis wind-turbine airfoil." *Energies* 12, no. 3 (2019): 488. https://doi.org/10.3390/en12030488